Deep Learning-Based System for Automatic Melanoma Detection

ADEKANMI A. ADEGUN[ID] AND SERESTINA VIRIRI[ID], (Member, IEEE)

School of Mathematics, Statistics and Computer Science, University of KwaZulu-Natal, Durban 4041, South Africa

Corresponding author: Serestina Viriri (viriris@ukzn.ac.za)

ABSTRACT Melanoma is the deadliest form of skin cancer. Distinguishing melanoma lesions from non-melanoma lesions has however been a challenging task. Many Computer Aided Diagnosis and Detection Systems have been developed in the past for this task. They have been limited in performance due to the complex visual characteristics of the skin lesion images which consists of inhomogeneous features and fuzzy boundaries. In this paper, we propose a deep learning-based method that overcomes these limitations for automatic melanoma lesion detection and segmentation. An enhanced encoder-decoder network with encoder and decoder sub-networks connected through a series of skip pathways which brings the semantic level of the encoder feature maps closer to that of the decoder feature maps is proposed for efficient learning and feature extraction. The system employs multi-stage and multi-scale approach and utilizes softmax classifier for pixel-wise classification of melanoma lesions. We devise a new method called Lesion-classifier that performs the classification of skin lesions into melanoma and non-melanoma based on results derived from pixel-wise classification. Our experiments on two well-established public benchmark skin lesion datasets, International Symposium on Biomedical Imaging(ISBI)2017 and Hospital Pedro Hispano (PH2), demonstrate that our method is more effective than some state-of-the-art methods. We achieved accuracy and dice coefficient of 95% and 92% on ISIC 2017 dataset and accuracy and dice coefficient of 95% and 93% on PH2 datasets.

INDEX TERMS Deep learning-based, encoding-decoding network, pixel-wise classification, melanoma, skin lesion, segmentation.

I. INTRODUCTION

Melanoma is a malignant itumour which develops from the pigment-containing cells known as melanocytes [1]. It has the most rapidly increasing mortality rate among skin cancers. The American Cancer Society [2] estimates that about 7,230 people are expected to die of melanoma and about 96,480 new melanomas is diagnosed in the United States in the year 2019. According to the statistics [2], the lifetime risk of getting melanoma is about 2.6% for whites, 0.1% for blacks, and 0.6% for Hispanics. Cutaneous melanoma is the most dangerous form of skin tumor that causes 90% of skin cancer mortality [3]. According to Garbe *et al.* [3] melanomas account for 90% of the deaths associated with cutaneous tumors. They also investigated that the incidence rate is around 25 new melanoma cases per 100,000 in Europe, and around 30 per 100,000 inhabitants in the United States

of America (USA) and in Australia where the highest incidence rate is observed it is around 60 per 100,000 inhabitants. The major and most important exogenous factor causing melanoma is exposure to UV irradiation through sun exposure [4]–[6]. Melanoma can however be cured with prompt excision [7], [8] if diagnosed and detected early. Identification of melanoma from skin lesions using methods such as visual inspection, clinical screening, dermoscopic analysis, biopsy and histopathological examination of skin lesion can be inaccurate and laborious even with experienced dermatologists [9]–[11]. This is due to the complex visual characteristics of the skin lesions such as multi-sizes, multi-shapes, fuzzy boundaries, low contrast when compared to the skin and noise presence such as skin hair, oils, air and bubbles. Development of an efficient Computer Aided Diagnosis (CAD) system for detection and diagnosis of melanoma cancer is thus requires. This will improve the diagnosis rate of melanoma and early detection which can facilitate treatment and reduce the mortality rate of the disease.

The associate editor coordinating the review of this manuscript and approving it for publication was Naveed Akhtar[ID].

A lot of optical techniques exist for melanoma screening. These techniques are non-invasive, with fast response and are sensitive to biochemical and structural changes presented in skin cancer development. They include wide-field imaging, optical spectroscopy and microscopy imaging [12]. The optical diagnostic systems are based on the one or more types of light-tissue interactions to provide both the biochemical and structural tissue information [13]–[15]. They are potential techniques for the identification of occult lesions using the conventional light examination [16]–[20], and also to serve as important auxiliary tools for clinical examination of skin [12]. The non-invasive skin cancer diagnostic methods have been categorized into photography, dermoscopy, sonography, confocal microscopy, Raman spectroscopy, fluorescence spectroscopy, terahertz spectroscopy, optical coherence tomography, the multispectral imaging technique, thermography, electrical bio-impedance and tape stripping [21], [22].

Pratavieira *et al.* [12] presented several optical modalities, including spectroscopy and imaging techniques as potential tools to improve cancer diagnostics. They also examined several commercial optical systems available such as Dermlite produced by 3Gen, LLC, Dana Point, CA, U.S.A., Dyaderm by Biocam GmbH, Regensburg, Germany, Dermascope by AMD Telemedicine, Elizabeth, NJ, U.S.A., MelaFind by Electro-Optical Sciences, Irvington, NY, U.S.A, Molemax by Derma Medical Systems, Vienna, Austria, Microderm by Visiomed Comp.,Bochum,Germany), Multiderm by Light4tech, Scandicci, Fi, Italy, Nevoscope by Translite LLC, Sugar Land, TX, U.S.A., Siascopy by Astron Clinica, Cambridge, UK, SolarScan by Polartechnics Ltd, Sydney, Australia, and many others. These devices have been specifically designed for the detection and interpretation of skin lesions but are however very limited in interrogation depth, photobleaching of biomolecules, and high signal background and also with high cost

There has been significant improvement in the research for the development of computing algorithms and techniques for skin lesion analysis in the recent past. Some of the popular techniques use a rule based on asymmetry, border structure, variegated colour and dermatoscopical structures (ABCD) [23]. This was derived from the rule commonly used by dermatologist for diagnosis of skin cancer. In the ABCD rule, asymmetry means that two sides do not match while they match for the symmetry. This can assist in distinguishing the benign from the malignant skin lesions [23]. The border structure may also be even for benign and uneven for the malignant in most cases. The variegated color is always just one color in the case of Benign while the malignant always possess two or more colors. The general dermatoscopical structure are always very small like one-quarter inch for the benign while is always larger than that in the case of malignant. The benign skin lesions are not harmful while the malignant are cancerous and harmful [24]. This rule has always been applied by many hand crafted methods for the analysis of skin lesions images towards the melanoma detection as shown in FIGURE 1.
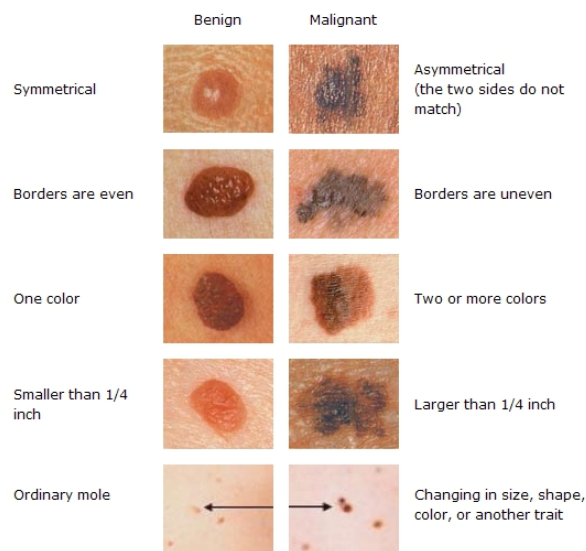

FIGURE 1. Images showing comparison between benign and malignant skin lesion using the ABCD rule. (drganesen.co.za/skin-lesions).

These methods termed hand-crafted are limited with the noise presence on the skin lesion and also the low contrast and irregular borders features of skin lesions [25]. These methods [26] lack deep supervision and this leads to loss of detailed information during training thus experience difficulty in analyzing the complex visual characteristics of the skin lesion. Intelligent based systems possess features such as adaptability, fault tolerance and optimal performance for better analysis of skin lesions [25]. Developing an efficient system will reduce the cost and time required for the dermatologists and doctors to diagnose all patients for melanoma [27]. Codella *et al.* [28] proposed a system that combines recent developments in deep learning with established machine learning approaches to create ensembles of methods that are capable of segmenting skin lesions for melanoma detection. Even though those methods have achieved great success, there still remain several challenges to the skin cancer segmentation task due to the complex nature of skin lesion images. Skin lesions images are characterized with fuzzy borders, low contrast between lesions and the background, variability in size and resolution and with possible presence of noise and artifacts.

In this paper, we propose an intelligent system based on deep learning techniques to detect and distinguish melanoma from non-melanoma lesions using a single DCNN for all the processes. Firstly, dermoscopy image may include hair, blood vessels, and other factors that interfere with segmentation. Moreover, the low contrast between the lesion area and the surrounding skin causes blurry boundary, which makes it difficult to segment the lesion accurately. At last, melanoma usually has different sizes, shapes, and colors depending on different skin condition, which could be a hamper to achieve high segmentation accuracy. To tackle

these challenges, we propose a novel CNN based approach with an enhanced deep supervised encoder-decoder network to extract strong and robust features of skin lesions images. This network is able to extract complex features from the lesion images through its multi-stage approach in which the encoder stage of the network learns the general appearance including possible hairs influence on the lesion region and localization information while the decoder stage learns the lesion boundaries characteristics. After extracting the features, a new method called Lesion-classifier is devised to perform the classification of skin lesions into melanoma and non-melanoma in a pixel-wise manner. Our network is distinguished from the existing methods based on the following three aspects: (1) we connect the encoder and decoder sub-networks together through a series of skip pathways as shown in Figure 3. This brings the semantic level of the encoder feature maps closer to that of the decoder feature maps is proposed to enhance the feature learning ability of the network and feature extraction; (2) we design a multi-scale system at each skip pathways of the network to handle various sizes of skin lesions images; (3) we devise a method called Lesion-classifier which is computationally efficient to classify skin lesions into melanoma and non-melanoma in a pixel-wise manner to distinguish melanoma lesions from non-melanoma images. The key innovation behind our proposed algorithm is that the melanoma detection task is structured as a point object detection task, where the region of interests (ROI) occupies only a tiny fraction of the total number of pixels of the skin lesion images. Our aim is to develop an efficient system that can extract the most suitable features using limited training images dataset and detect melanoma cancer with reduced computing resources that can meet up with the requirement in the real-time clinical practice.

Our last contribution is experimental. We present a more detailed study, with better visualizations of the results and outputs. The proposed system obtains state-of-the-art results on ISIC 2017 and PH2 datasets and show better results than the existing techniques in major performance metrics in recognition and localization. The proposed methodology archives encouraging results having 96% accuracy. We finally experimentally evaluate the training computation time per epoch and the test time per a single dermoscopy image for the proposed method and compare the results with the performance of some popular deep learning methods such as SegNet, UNet and FCN on ISBI 2017 dataset.

A. OUR APPROACH

We propose a new fully automated method for detecting melanoma on dermoscopic images. Experiments show that the proposed method improves on the state-of-the-art and is specifically optimized for melanoma detection. The system employs an end-to-end and pixel by pixels supervised learning approach using Deep Convolutional Networks combined with softmax classifier and dice loss function. In addition to this, we contrive a method to classify skin lesions into melanoma and non-melanoma based on pixel-wise result

from the softmax module. This model combines all the challenging tasks of segmentation, features extraction and classification in a manner that no extra computing cost is required. Our research aims at improving the rate and accuracy in identifying and classifying skin lesions. The following contributions have been introduced to the present state-of-the-art:

1) DEEP CONVOLUTIONAL ENCODER-DECODER ARCHITECTURE

We propose a Deep Convolutional Architecture that is interconnected through a series of skip pathways as shown in Figure 3. This brings the semantic level of the encoder feature maps closer to that of the decoder feature maps is proposed to enhance the feature learning ability of the network and feature extraction;

2) MULTISTAGE AND MULTI-SCALE APPROACH

The Encoder-Decoder network is enhanced into a moderate size with a multi-stage and multi-scale approach to enhance learning of the complex features and handle various sizes of skin lesions images;

3) LESION-CLASSIFIER

We devise a new predictive method called Lesion-classifier which is computationally efficient to classify skin lesions into melanoma and non-melanoma in a pixel-wise manner to distinguish melanoma lesions from non-melanoma images using the output of the softmax modules.

Our method is particularly effective for analysing challenging skin lesions, which usually have fuzzy boundaries and heterogeneous textures, for melanoma detection.

The remaining part of this work is organized as follows: Section II discusses the Related Works and Materials and Methods is described in Section III. Section IV discusses the Experiments and Results. The paper is concluded in Section V.

II. RELATED WORKS

An efficient automatic melanoma detection system requires a reliable feature extraction mechanism. This process is of vital importance while detecting melanoma using CAD diagnostic systems. In the recent past decade various methods have been proposed to extract and analyse various features from skin lesion images. Extracted features include but not limited to colour, Texture wavelet, gray-level co-occurrence matrix (GLCM) and shape features. The performance of any CAD system is highly dependent on the efficiency of the extraction of these features. Many semi-automatic and fully-automatic algorithms have been proposed for melanoma detection from skin lesions images. This section describes both the semi-automatic techniques and automatic deep learning methods for features extraction and melanoma detection.

A. SEMI-AUTOMATIC TECHNIQUES

Warsi *et al.* [29] presented a technique based on D-optimality orthogonal matching pursuit (DOOMP) to

perform image enhancement, segmentation, and classification on skin lesions using fixed wavelet grid network (FWGN). The system gave accuracy results of 91.82%. Barata *et al.* [30] also used a technique to extract both color and texture features for detection of melanoma and non-melanoma images. The method showed that color feature outperforms the texture feature. Schaefer *et al.* [31] also proposed a method to extract color and texture features from the lesion component of dermoscopic images. The proposed method used the combination of SVM, SMOTE, and ensemble of classifiers. The results of the proposed ensemble classifier system gave accuracy of 93.83%. Waheed *et al.* [32] extracted both the color and texture features using GLCM method for texture feature extraction and SVM classifier for classification. The system obtained the accuracy of 96%. Sivaraj *et al.* [33] used Firefly with K-Nearest Neighbor algorithm (FKNN) classifier to predict and classify skin cancer along with threshold-based segmentation and ABCD feature extraction algorithm. Pennisi *et al.* [34] presented a method based on Delaunay triangulation known as ASLM to extract a binary mask of the lesion. This method combines two parallel processes for detection of skin and lesion. Warsi et al designed a method termed multi-direction 3D color-texture feature (CTF) for feature extraction from dermoscopic images. They used back propagation multilayer neural network (NN) classifier for detection and classification of melanoma [29]. The shortcomings of these methods include requiring elaborate image pre-processing steps, careful initialization from a human expert and also too slow for real-time analysis and diagnosis. These techniques do not however include a prior knowledge of the image characteristics in the algorithm unlike approaches based on deep learning algorithms.

B. AUTOMATIC DEEP LEARNING TECHNIQUES

Recently, Convolutional Neural Network (CNN) and deep learning-based approaches have been used for cancer detection. Bi *et al.* [35] proposed an automatic melanoma detection technique for dermoscopic images using multi-scale lesion-biased representation (MLR) and Joint reverse classification (JRC). JRC model was used for classification and it provided additional information for melanoma detection. PH2 public database wass used for evaluation and testing of the proposed method. The results gave 92% accuracy. Yıldız [36] designed a deep neural network model named C4Net for melanoma detection. The proposed model classified skin lesions into malignant and benign. Abbes and Sellami [37] proposed a model based on the ABCD rule for features extraction and used Fuzzy C-Means(FCM) to determine membership degree and finally used a deep neural network classifier for decision making. The model gave 87.5% accuracy as result. A pre-trained deep learning network and transfer learning are utilized for skin lesion classification by Hosny *et al.* [38] Transfer learning was applied to AlexNet by replacing the last layer with softmax to classify the lesions. Finally, a single CNN was utilized and trained end-to-end from images using

only pixels and disease labels as inputs [39]. This was used for binary classification of keratinocyte carcinomas versus benign seborrheic keratoses; and malignant melanomas versus benign nevi. The deep learning CNN outperforms the average of the dermatologists at skin cancer classification using photographic and dermoscopic images however the performance in a real-world and clinical setting is yet to be evaluated [39]. The computation cost for these approaches are major barriers in clinical applications [40]–[42]

Al-Masni *et al.* [43] proposed a method that learns the full resolution features of each individual pixel of an input data directly. The system was evaluated using two publicly available databases,ISBI 2017 Challenge and PH2 datasets. He *et al.* [44] presented a skin lesion segmentation network using a very deep dense deconvolution network. They employed the combination of deep dense layer and generic multi-path Deep RefineNet. Esteva *et al.* [39] developed CNN architecture using GoogleNet Inception v3 that was pre-trained on approximately 1.28 million images for melanoma detection. Goyal and Yap [45] presented an end-to-end solution using fully convolutional networks (FCNs) for multi-class semantic segmentation. The system automatically segmented the melanoma into keratoses and benign lesions. Ramachandram and Devries [46] proposed a semantic segmentation architecture that utilized atrous convolutions for super-resolution upsampling of predictions using subpixel. A deep learning framework consisting of two fully-convolutional residual networks (FCRN) was developed to simultaneously produce the segmentation result and the coarse classification result of skin lesion [47]. A lesion index calculation unit (LICU) was then developed to refine the coarse classification results by calculating the distance heat-map.

Our proposed system aims at lowering trainable parameters to reduce computational resources and time and make the system feasible for real-time medical diagnosis. Most of the systems discussed above employ larger and more complex deep learning architecture. Our proposed system is able to perform both segmentation and pixel-wise classification of melanoma lesion pixels using a moderate-size deep convolutional network. Some of these methods are also too slow and requires huge amount of computing processing resources for real-time medical analysis and diagnosis.

III. MATERIALS AND METHODS
A. MATERIALS
In this work, two publicly available dermoscopy dataset were utilized for training and testing of our proposed method. These were used to evaluate the proposed method. The first dataset is the ISIC 2017 challenge dataset. This dataset is extracted from the International Skin Imaging Collaboration (ISIC) archive. The dataset contains dermoscopy images with different image sizes with the highest resolution of 1022×767. 2000 dermoscopy images and 600 dermoscopy images were used for training and
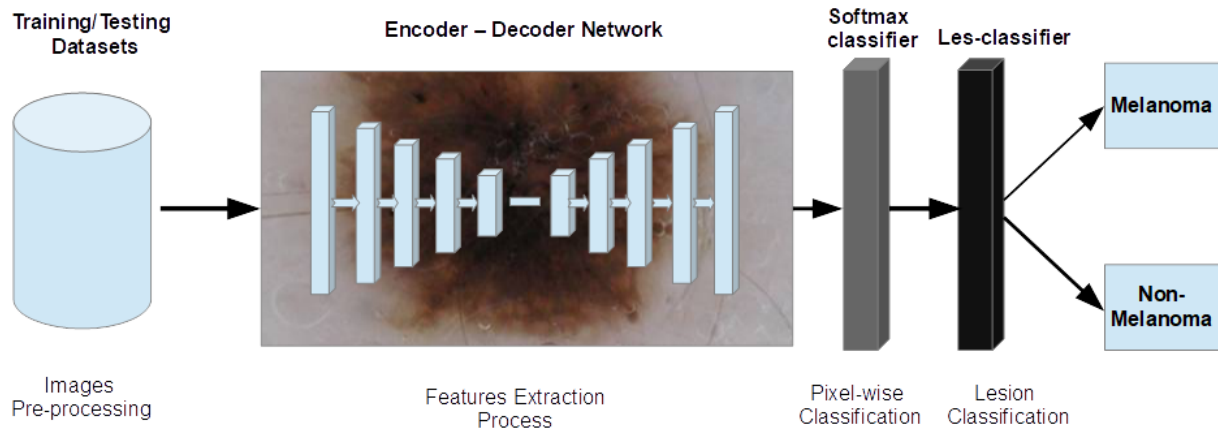
testing respectively. These images were also presented with their respective ground truth labels for supervised training. The second dataset is the PH2 images. The dataset contains dermoscopy images with different image sizes with highest resolution of 765×574 pixels. The images were collected from the Dermatology centre of Hospital Pedro Hispano. 200 dermoscopy images and 60 dermoscopy images were used for training and testing respectively. They are also presented with their corresponding ground truth labels based on manual delineations by clinical experts.

B. OVERVIEW OF THE PROPOSED METHOD

The diagram in Figure 2 shows all the major stages from image-preprocessing to features extraction and pixel-wise classification and finally lesion classification. The major components include skin lesions images datasets, Encoder-Decoder Network, Softmax classifier and lesion classifier. The image datasets were first pre-processed before being sent into the Encoder-Decoder Networks. The training dermoscopic images together with the ground truth labels (annotations) are used in training the Deep Convolutional Encoder-Decoder Networks. The input is first sent into the encoder sub-network and then to the the decoder for features extraction. An additional module that combines the dice loss function with the softmax classifier is later used for pixel-wise classification of the images and identification of Region of Interest for melanoma. During the testing stage, we also applied the Deep Convolutional Encoder-Decoder Networks to the input dermoscopic image dataset. The full architectural diagram of the Encoder-Decoder Network is shown in Figure 3.

C. DATA PRE-PROCESSING AND IMAGE AUGMENTATION

The skin lesions images are often characterized with noise and artefacts such as air, hair and bubbles. They are also characterised with variation in size and multi-scale and multi-resolution nature features of the skin lesion images. During the pre-processing stage the images are separated from noise using the Gaussian filter. The function is stated below. This smoothens and prepares the images for further processing. The images are also prepared to have them in the same scale and resolution via cropping, resizing and re-sampling. In this work, we use relatively small image size of 224×224. This will reasonably reduce the input feature map size for the network. The images are normalized by computing the mean pixel value and the standard deviation for data centring data normalization. The system applied elastic deformations through random displacements before augmenting the dataset. Elastic deformation utilizes local distortion and random affine transformation for high-quality output. These transformation takes place with random displacement. In addition, simple and random rotation is adopted in the augmentation process to improve the performance. The system centres the pixel intensity ranging around zero by remapping intensities linearly to the range $[-0.5, 0.5]$ to provide numerical stability during training.

D. ROI IDENTIFICATION AND FEATURES EXTRACTION

In the process of detecting melanoma, identification of region of interest (ROI) and features extraction are very important tasks. A lesion is characterized by different features including colour, texture etc. In this work, an efficient deep learning framework with a medium-size and less trainable weight of the encoder-decoder network is trained and adapted for features extraction. Both encoding part and the decoding part are made up of five blocks each.

Each block in the encoding part is composed of two 3×3 convolutional layers and one max pooling layer and a RELU non-linear activation function for features extraction. The max-pooling module breaks down the input feature maps into pooling sections, and computes the maximum of each section. The max-pooling module pools over every pixel
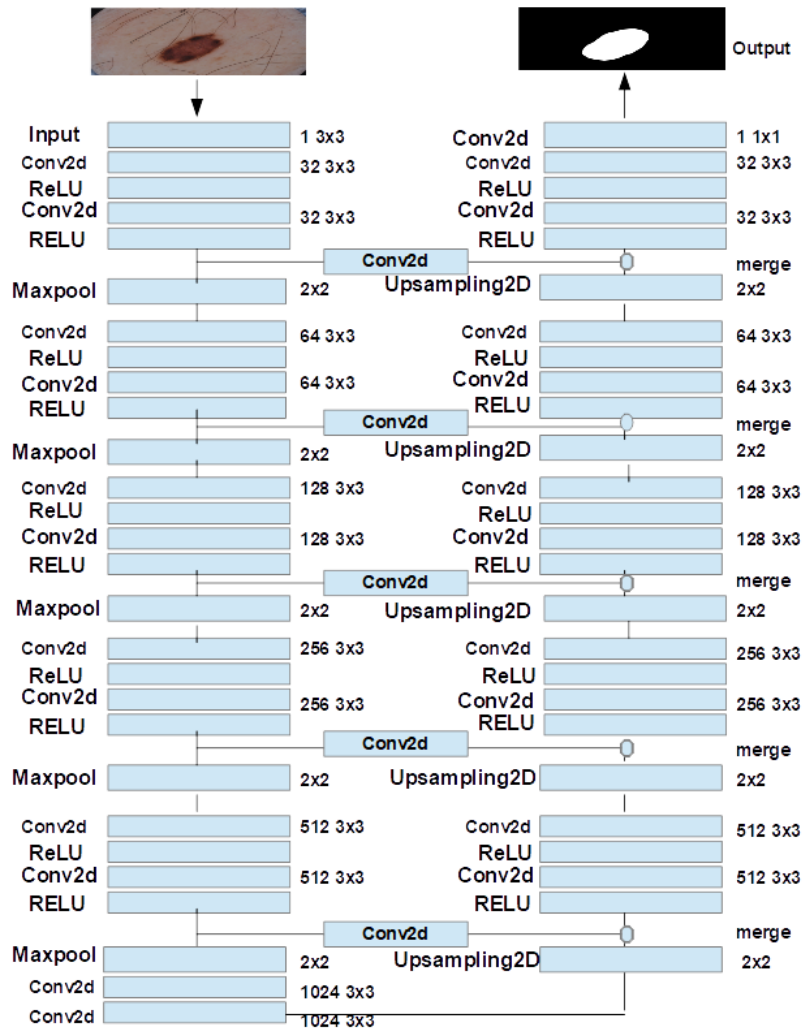
FIGURE 3. Achitectural diagram for deep convolutional encoder-decoder network.

within a 2×2 area from the feature map and reduces the feature map's size and resolution. This eliminates features redundancy and minimizes computation time. This also facilitates learning process in the network.

$$F_i = ReLU(W * F_i - 1 + b_i) \tag{1}$$

where F_i is the feature map, $F_i - 1$ is the feature map for the previous layer, W is the filter kernel and b_i is the bias applied to each feature map of each layer. The ReLU activation function is stated as:

$$U(y) = max(0, y) = \begin{cases} y & \text{if } y \geq 0 \\ 0 & \text{if } y < 0 \end{cases}$$

where y is the resulting feature map.

Encoder learns lesion image pattern via the convolutional layers and the ReLU activation function during an end-to-end and pixel by pixel system training process. The first convolution layer extracts feature maps from the training dataset. The encoder captures the semantic and contextual information of the lesions by learning the general appearance and localization information of the input image. Our architecture is a deeply-supervised encoder-decoder network where the encoder and decoder sub-networks are connected through a series of skip pathways. This series of skip pathways is composed of convolutional networks and short skip network. This brings the semantic level of the encoder feature maps closer to that of the feature maps awaiting in the decoder for efficient and faster processing.

The decoder part also consists of five units but with each units composing two convolutional layers and one up-sampling layer. In the decoding part, the previous block output is upsampled with the nearest neighbour using a 2×2 convolutional layers. It is then concatenated with the output from the encoder part at the corresponding level. Increase in deep learning network size automatically increases the computational cost and reduce the feasibility of the system in medical diagnosis. So in this work we limited the size of the encoder-decoder network. The network has however been optimized by replacing the usual skip network connection

between the encoder subnetwork and decoder subnetwork with a series of skip pathway as illustrated in Figure 3. The up-sampling layer is concatenated with the corresponding feature map from the convolutional layer in the encoder part. Feature maps are convolved with the decoder filters in the convolutional layers to produce dense feature maps. The lesion boundaries localisation information is learned at the decoder section. The decoder section learns the characteristics of the lesion boundaries in recovering spatial information. The decoders work to restore the feature maps to the original size in the network using the upsampling layers with the function stated below.

$$y = upsample(x, n) \tag{2}$$

where x is the feature map from the encoder and n is the upsampling layer input.

The upsampling module is an advanced technique of unpooling that reverts maxpooling operation by using the value and location of the maxima values in the maxpooling layers for feature maps restoration.

1) SYSTEM ALGORITHM

Algorithm 1 shows the steps of the proposed model implementation. The algorithm first gets an input image X, feature maps are generated and then sent into encoder-decoder system before pixel-wise classification with softmax classifier, and finally obtain the classification result via the Lesion-Classifier. In the encoder unit, the feature maps generated, F_{map}, is first sent to the convolutional layers as $Conv(F_map)$ and then to the ReLu activation function as $Relu(F_ci)$. This is then down-sampled with the max-pooling function, $Pooling(F_ri)$. This is done through the for loop structure until all the images are processed. The output from the encoder is then sent into the decoder. It passess into the for loop structure and goes through features upsampling using the upsampling function $Upsamp(F_pi)$. This is also sent into the ReLU activation function and the convolutional layers.

E. PIXEL-WISE CLASSIFICATION

The pixel-based classification as presented by Wu *et al.* [48] has been employed in the pixel-wise classification of skin lesions. The encoder-decoder trains skin lesion images from end-to-end and pixels to pixels using pixels and disease labels to produce pixel-wise prediction. The output from the encoder-decoder network with high dimensional feature representation is sent into a trainable soft-max classfier. The softmax performs the classification where n represents the number of classes to specifically predict the class for each pixel as melanoma or non-melanoma. The Dice loss function utilizes Dice similarity coefficient [49] to measure overlap between the input image and the corresponding ground truth. These are explained by the equations below.

$$P(y = i|x) = \frac{e^{x^T w_i}}{\sum\limits_{n=1} e^{x^T w_n}} \tag{3}$$

Algorithm 1 Proposed Model for the Deep Convolutional Encoder-Decoder Network

1: **procedure** Encoder(X)   ▷ X: x (L, B, H) is an input image with dimension L, B, H
2:     Extract the feature map F_map from the input image;
3:     For $i = 0$ to M-1:
4:         Set $F_{ci} = Conv(F_{map})$;
5:         Set $F_{ri} = Relu(F_{ci})$;
6:         Set $F_{pi} = Pooling(F_{ri})$;
7:         if $i <= M$ then
8:         Set $F_{pi+1} = F_{pi}$;
9:         else return F_{pi}
10:        end if
11:    end for
12: **procedure** Decoder(F_{pi})   ▷ F_{pi} is the downsampled feature maps
13:     For $i = M-1$ to 0:
14:         Set $F_{di} = Upsamp(F_{pi})$;
15:         Set $F_{ri} = Relu(F_{di})$;
16:         Set $F_{ci} = Conv(F_{ri})$;
17:         if $i <= M$ AND $i != 0$ then
18:         Set $F_{pi-1} = F_{ci}$;
19:         else return F_{ci}
20:        end if
21:    end for
22: Predictedpixels= softmaxclassifier(F_{ci})   ▷ F_{ci} which is the output from the decoder is sent to softmax classifier function for pixel-wise prediction
23: Pi= cluster(Predictedpixels)   ▷ The predicted pixels are clustered into segmented output
24: Finalresults= Pi   ▷ Final Segmented Output Display Finalresults

---

where $x^T w$ represents the product of x and w, x is the feature map and w is the kernel operator.

where xTw represents the product of x and w, x is the feature map and w is the kernel operator.

Applying Dice loss functions in this system results in better performance of the proposed model. This loss function is efficient with skin lesion images due to the low contrast characterisics of skin lesions images, with the dice loss function differentiating the background from the lesion itself. Dice loss function computes the losses for each class separately and then find the average [50] to yield a final score. Incorporating dice loss function will create a function that returns the dice loss between the predictions made and the training targets and utilize this difference to improve the performance.

$$DiceLoss = 1 - \frac{2 \sum_i Y_t Y_p}{\sum_i Y_t^2 + \sum_i Y_p^2} \tag{4}$$

where i is the pixels, Y_t denotes the ground truth label, Y_p denotes the predicted image output. This can be further expressed as:
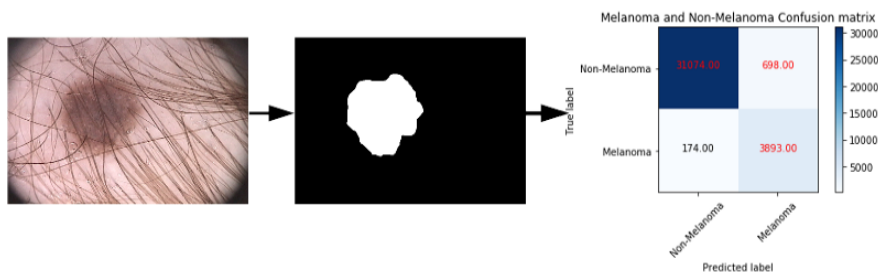
$$Loss = forwardloss(layer, Y, T) \tag{5}$$

FIGURE 4. Pixel-wise classification of a Melanoma lesion.

where Y is the output of the previous layer and T represents the training targets.

The Softmax classifier provides and compute the probabilities with direct interpretation for all labels. Our results are presented using confusion matrix as illustrated in Figure 4 where True positives, TP, represent pixels in which the prediction and actual value are melanoma. True negatives, TN, are pixels captured when the actual and predicted value is Non-Melanoma. False negatives, FN, represent pixels, where the pixel's prediction is non-melanoma and the actual category is melanoma. Finally, false positives, FP, capture pixels, where the prediction is melanoma and the actual category is non-melanoma.

F. SKIN LESION CLASSIFICATION

Algorithm 2 shows the steps of the proposed model implementation. The algorithm first gets an input image X, feature maps are generated and then sent into encoder-decoder system before pixel-wise classification with softmax classifier, and finally obtain the classification result via the Lesion-Classifier. In the encoder unit, the feature maps generated, F_map, is first sent to the convolutional layers as $Conv(F_map)$ and then to the ReLu activation function as $Relu(F_ci)$.

Algorithm 2 Lesion Classifier Algorithm for Detecting the Number of Melanoma Lesions

1: Set *MelClass* = 0;
2: Set *NonMelClass* = 0;
3: **procedure** LesionClassifier(X)   ▷ X: x (L, B, H) is an input image
4:      Accept Set of Images as Input;
5:      For *imagecount* = 0 to $M - 1$:
6:      Extract MelPixelsNo From Softmax modules;
7:      if *MelPixelsNo* > 0 then
8:      Set *MelClass* = *MelClass* + 1;
9:      else
10:     Set *NonMelClass* = *NonMelClass* + 1;
11:     end if
12:     end for
13:     return *MelClass*

Lesion Classification Algorithm

IV. EXPERIMENTS AND RESULTS

Various experiments were carried out in this section to evaluate the performance of our proposed segmentation approach. Two publicly available dataset were used to demonstrate our proposed methods. This was also compared with the existing algorithms in Table 1 and 2.

TABLE 1. Segmention Performance(%) of the proposed model on ISIC Datatest.

Techniques	Accuracy	Dice Score	Sensitivity	Specificity
Proposed model	**95**	**92**	**97**	**96**
FrCN [44]	95	91	93	95
U-NET [44]	92	87	81	97
FCN [44]	93	89	80	94

TABLE 2. Segmention Performance (%) of the proposed model on PH2 Datatest.

Techniques	Accuracy	Dice Score	Sensitivity	Specificity
Proposed model	**95**	**93**	**93**	**95**
FrCN [44]	95	91	93	95
FCN [44]	92	89	90	94
U-NET [44]	92	87	81	97

A. DATASETS

The two well-established publicly available datasets used in the evaluation of the proposed segmentation method are from the ISIC challenge in skin lesion segmentation and PH2 data repository. They are described below:

1) PH2

PH2 [51] contains 200 skin lesion images with highest resolution of 765×574 pixels. They were gotten at Dermatology Service of Hospital Pedro Hispano. This dataset was categorized into training and testing image set both comprising of images and ground truth labels respectively. The input dataset are skin lesion images in JPEG format while the ground truth are mask image in PNG format.

2) ISIC

ISIC 2017 [52] contains 2000 training images with the ground truth provided by experts. The image sizes possess highest resolution of 1022×767. This dataset was provided from the ISIC Dermoscopic Archive [52]. This dataset was categorized

into training and testing image set both comprising of images and ground truth labels respectively. The input dataset are skin lesion images in JPEG format while the ground truth are mask image in PNG format. The ground truth labels are provided for training and evaluating validation and test phases data using the performance evaluation metrics.

B. MODEL IMPLEMENTATION

The experimental platform is on LENGAU clusters hosted on CHPC super computers server at chpc.ac.za. Hardware resources with an Intel Core i7 processor with ten (10) 3.4 GHZ cores and NVIDIA Tesla K40c GPU, 148.5 TB shared memory was utilized.

Training time taken for the experiments: 4hrs

The software used for the model implementation includes:

- Python Version 3.5.2
- Keras 2
- Tensor flow backend 1.1.0 and TFlearn 0.3
- Scikit-image Version 0.14.1

C. CALCULATION METRICS

The most common skin lesion segmentation evaluation metrics were used for comparison including: dice similarity coefficient (DSC.), sensitivity, specificity and accuracy. These metrics were used for evaluation of the model. They are illustrated below:

Dice Similarity Coefficient: It measures the similarity or overlap between the ground truth and the automatic segmentation. It is defined as

$$DSC = \frac{2TP}{FP + 2TP + FN} \qquad (6)$$

Sensitivity: It measures the proportion of those with positive values among those who are actually positive.

$$Sensitivity = \frac{TP}{TP + FN} \qquad (7)$$

Specificity: This is the proportion of those that are negative among those who actually tested negative.

$$Specificity = \frac{TN}{TN + FP} \qquad (8)$$

Accuracy: It measures the proportion of true results (both true positives and true negatives) among the total number of cases examined.

$$Accuracy = \frac{TP + TN}{TP + TN + FP + FN} \qquad (9)$$

where *FP* is the number of false positive pixels, *FN* is the number of false negative pixels, *TP* is the number of true positive pixels and *TN* is the number of true negative pixels.

D. RESULTS AND DISCUSSION

With regard to melanoma lesion detection and segmentation process, the proposed system was evaluated on two publicly available database. First, the proposed model was trained on ISIC 2017 dermoscopic dataset with 2000 training skin lesion images. This was then tested on 200 skin lesion images. The result achieved accuracy and dice coefficient of 95% and 92% respectively with training steps of 35 epochs as shown Figure 5 and 6. Training the proposed model on PH2 skin lesion image dataset requires more number of training steps because of the dataset size of 200 images. The model was also tested on 50 images. As shown in Figure 5 and 6, the result achieved accuracy and dice coefficient of 95% and 93% with 250 training epochs on PH2.

The results displayed in Figure 5 and 6 for both ISIC 2017 and PH2 dataset also show that the accuracy and the dice score can still improve with increase in training steps and dataset. The learning ability of the proposed model through experiments with the two datasets was evaluated with the accuracy curve in figure 5. The result from the curve clearly shows that the ISIC 2017 dataset with fairly large dataset reached the accuracy percentage of 95%. This improvement can be due to the adopted dice loss function with the softmax classifier.
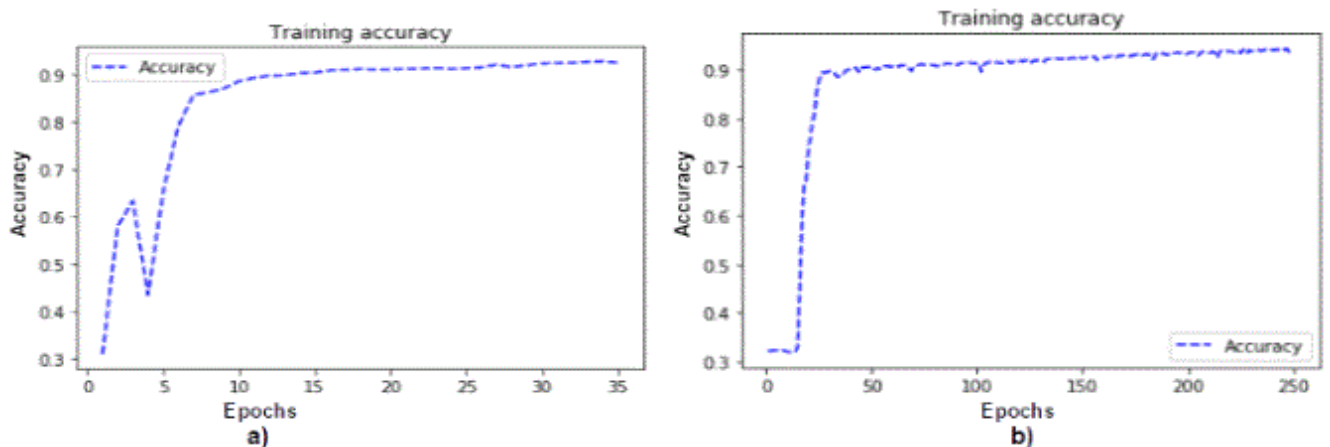
FIGURE 5. Training Accuracy Curves of the proposed method on the two datasets: a) ISIC b) PH2.
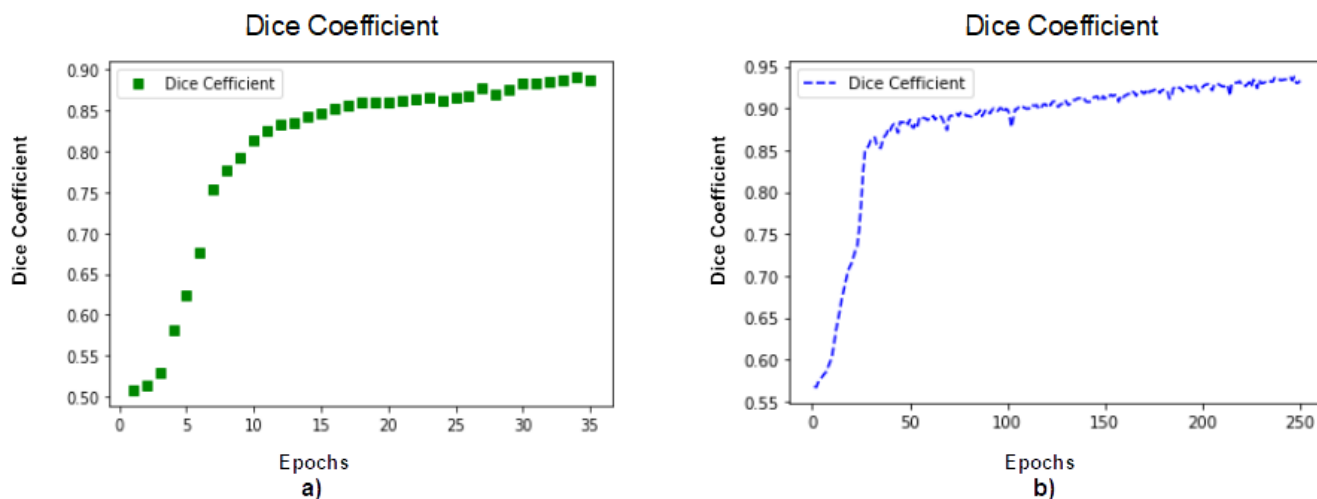
FIGURE 6. Dice Coefficient Curves of the proposed method on the two datasets: a) ISIC b) PH2.
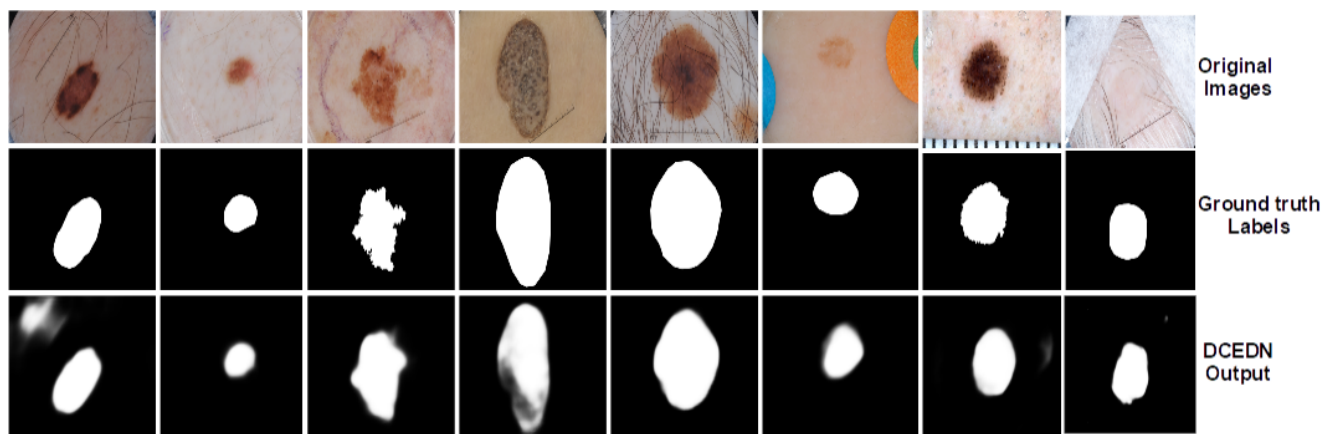

FIGURE 7. Segmentation Results of the proposed method on ISBI 2017 dataset: The first row shows the Input images; the second rows shows the Ground truth labels; the third row shows Segmented Output on DCEDN only.

We compared the performance of the proposed model with the performance of some state-of-the-art methods from the latest study in literature such as FrCN, CDNN, FCN and UNET. This was carried out on the two datasets ISIC 2017 and PH2 and the results are stated in Table1 and Table2. The results show that the proposed model outperform some of the state-of-the-arts. From the results in Table 1, the proposed model records higher accuracy percentage and dice score of 95% and 92% on ISIC 2017 dataset when compared with other methods. It also shows higher sensitivity and specificity of 97% and 96% as against the other methods.

From the results in Table 2, the proposed model also gives higher accuracy percentage and dice score of 95% and 93% on PH2 dataset when compared with other methods. It also shows high sensitivity and specificity of 93% and 95% as against some of the methods. This results again indicates that the proposed system is able to identify and differentiate higher number of affected skin lesions from the healthy tissues on PH2 skin lesion dataset.

Table 1 shows the performance evaluation of our proposed method on ISIC 2017 Dataset and then compared with other state-of-the-art algorithms while Table 2 shows the performance evaluation of our proposed method on PH2 skin lesion dataset also compared with other state-of-the-arts methods. We use the same comparison algorithms but different databases in the two table. In Table 1, our proposed method and other state-the-arts methods were experimented on ISIC 2017 dataset while in Table 2 our proposed method and other state-the-arts methods were experimented on PH2 dataset.

Table 3 shows the performance evaluation of our proposed method on ISIC 2017 Dataset and then compared with the best three models in ISIC 2017 challenge as stated below.

The robustness and effectiveness of the proposed method is further shown in the Figure 7 with Deep Convolutional Encoder Decoder Network (DCEDN) architecture producing segmentation output with well defined lesion boundaries and contours for eight sample melanoma lesion images.
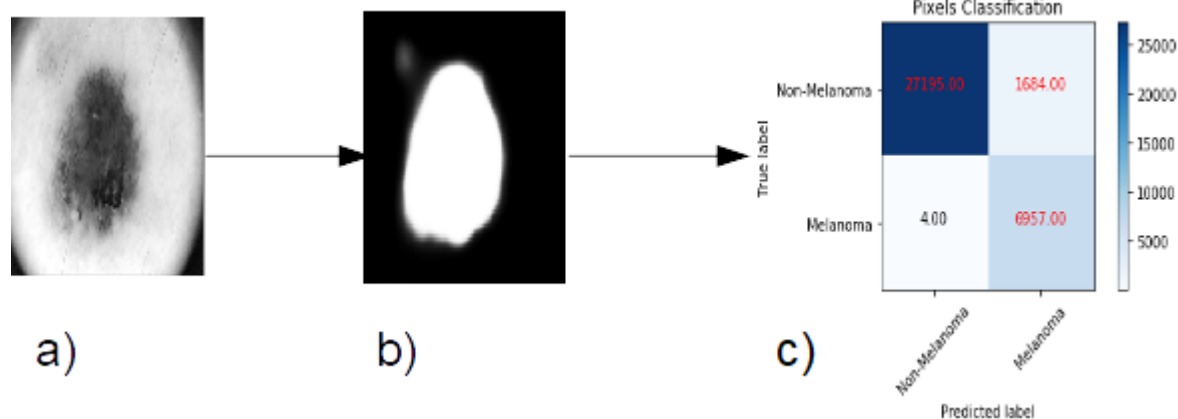
FIGURE 8. Segmentation Process and Per-pixel Results from the proposed method using Confusion matrix for result presentation: 27150 pixels are non-melanoma pixels that is correctly classified as non-melanoma and 6957 pixels are melanoma pixels correctly classified as melanoma.

TABLE 3. Segmention Performance(%) of the proposed model compared with the best three performance models in ISIC 2017 Challenge.

Techniques	Accuracy	Dice Score	Sensitivity	Specificity
Proposed model	**95**	**92**	**97**	**96**
CDNN [55]	93	85	83	97
U-NET [55]	93	85	82	97
ResNet [55]	93	84	80	98

Figure 8 shows the the pixel-wise results output using confusion matrix of a sample melanoma lesion image with 6957 pixels that are melanoma and predicted to be melanoma. It also discovers 27195 pixels of non-melanoma pixels predicted to be non-melanoma.

We have investigated both training and experimental time for further evaluation of the proposed model. The training computation time per epoch and the test time per a single dermoscopy image for the proposed method have been evaluated. The proposed system was evaluated on ISIC 2017 with 2000 training images over a total number of 35 epochs. It takes approximately 350s for training each epoch and the test time per a single image is around 5s. The proposed method is feasible for medical practices since the processing can be done in averagely 5s of processing time for each dermoscopy image. This result was compared with the performance of some segmentation methods such as SegNet, UNet and FCN. The evaluation was done under the same hardware conditions, the same dataset and the same number of epochs and the result presented in Table 4. The computational speed during the training phase of our proposed method was faster than other segmentation methods.

TABLE 4. Measurements in seconds of the training time per epoch and test time per skin lesion image.

Techniques	Training Time/ epoch	Test Time/Image
Proposed model	**350**	**5**
FCN	650	15
UNET	450	10
SegNet	600	13

V. CONCLUSION

In this paper, a deep convolutional network based architecture has been proposed for robust detection and segmentation of melanoma lesions. This architecture adopts an enhanced deep convolutional network that is interconnected with series of skip pathway. It also employs a reduced-size encoder-decoder network that aims at minimizing the computational resources consumption. The multi-stage approach overcomes the limitation of some deep convolutional networks in producing coarsely segmented outputs when processing challenging skin lesion images. In this approach, the whole network is divided into stages, with each stage handling different section of features learning and extraction. A new method is devised to classify melanoma and non-melanoma lesion based on the results from the softmax classifier. The system adapts dice loss function that learns and computes losses from the overlap in-between the predicted output and the ground truth label into softmax classifier for pixel-wise classification. This loss function consumes lesser system resources since it does not perform sample re-weighting unlike some other loss function. The system aims at reducing deep learning architecture complexity in detecting melanoma. It also aims at developing an efficient system that can meet up with real time medical diagnosis task in diagnosing melanoma cancer. The proposed method is feasible for medical practices with the processing time for each dermoscopy image at averagely 5s. The system was evaluated on two publicly available skin lesion image dataset. The proposed system achieved an overall accuracy and dice coefficient of 95% and 92% on ISIC 2017 dataset and accuracy and dice coefficient of 95% and 93% on PH2 dataset. Our proposed method outperforms some existing state-of-the-arts.

REFERENCES

[1] National Cancer Institute, PDQ Melanoma Treatment. Bethesda, MD, USA. (Nov. 4, 2019). *PDQ Adult Treatment Editorial Board*. Accessed: Dec. 9, 2019. [Online]. Available: https://www.cancer.gov/types/skin/hp/melanoma-treatment-pdq

[2] Cancer Statistics Center. (2019). *American Cancer Society*. [Online]. Available: https://cancerstatisticscenter.cancer.org

[3] C. Garbe, K. Peris, A. Hauschild, P. Saiag, M. Middleton, L. Bastholt, J.-J. Grob, J. Malvehy, J. Newton-Bishop, A. J. Stratigos, H. Pehamberger, and A. M. Eggermont, "Diagnosis and treatment of melanoma. European consensus-based interdisciplinary guideline—Update 2016," *Eur. J. Cancer*, vol. 63, pp. 201–217, Aug. 2016.

[4] J. A. Curtin, T. Fridlyand, T. Kageshita, H. N. Patel, K. J. Busam, and H. Kutzner, "Distinct sets of genetic alterations in melanoma," *New England J. Med.*, vol. 353, no. 20, 2005, Art. no. 2135e47.

[5] J. A. Curtin, K. Busam, D. Pinkel, and B. C. Bastian, "Somatic activation of KIT in distinct subtypes of melanoma," *J. Clin Oncol.*, vol. 24, no. 26, pp. 4340–4346, Sep. 2006.

[6] H. Tsao, M. B. Atkins, and A. J. Sober, "Management of cutaneous melanoma," *New England J. Med.*, vol. 351, no. 10, 2004, Art. no. 998e1012.

[7] M. E. Celebi, H. A. Kingravi, B. Uddin, H. Iyatomi, Y. A. Aslandogan, W. V. Stoecker, and R. H. Moss, "A methodological approach to the classification of dermoscopy images," *Computerized Med. Imag. Graph.*, vol. 31, no. 6, pp. 362–373, Sep. 2007.

[8] G. Capdehourat, A. Corez, A. Bazzano, R. Alonso, and P. Musé, "Toward a combined tool to assist dermatologists in melanoma detection from dermoscopic images of pigmented skin lesions," *Pattern Recognit. Lett.*, vol. 32, no. 16, pp. 2187–2196, Dec. 2011.

[9] M. E. Celebi, H. Iyatomi, W. V. Stoecker, R. H. Moss, H. S. Rabinovitz, G. Argenziano, and H. P. Soyer, "Automatic detection of blue-white veil and related structures in dermoscopy images," *Computerized Med. Imag. Graph.*, vol. 32, no. 8, pp. 670–677, Dec. 2008.

[10] Q. Abbas, M. Celebi, C. Serrano, I. F. N. García, and G. Ma, "Pattern classification of dermoscopy images: A perceptually uniform model," *Pattern Recognit.*, vol. 46, no. 1, pp. 86–97, Jan. 2013.

[11] A. Adegun and S. Viriri, "An enhanced deep learning framework for skin lesions segmentation," in *Proc. Int. Conf. Comput. Collective Intell.* Cham, Switzerland: Springer, 2019, pp. 414–425.

[12] S. Pratavieira, C. T. Andrade, A. G. Salvio, V. S. Bagnato, and C. Kurachi, "Optical imaging as auxiliary tool in skin cancer diagnosis," in *Skin Cancers-Risk Factors, Prevention Therapy*, May 2012, pp. 159–173.

[13] N. E. Marcon, R. S. DaCosta, and B. C. Wilson, "Fluorescence and spectral imaging," *Sci. World J.*, vol. 7, pp. 2046–2071, 2007.

[14] N. Ramanujam, "Fluorescence spectroscopy of neoplastic and non-neoplastic tissues," *Neoplasia*, vol. 2, nos. 1–2, pp. 89–117, Jan./Apr. 2000.

[15] A. A. Marghoob, L. D. Swindle, C. Z. Moricz, F. A. S. Negron, B. Slue, A. C. Halpern, and A. W. Kopf, "Instruments and new technologies for the *in vivo* diagnosis of melanoma," *J. Amer. Acad. Dermatol.*, vol. 49, no. 5, pp. 777–797, Nov. 2003.

[16] P. Carli, V. De Giorgi, and B. Giannotti, "DermoscDermoscopy and early diagnosis of melanoma: The light and the dark," *Arch. Dermatol.*, vol. 137, no. 12, pp. 1641–1644, Dec. 2001.

[17] A. Bono, S. Tomatis, C. Bartoli, G. Tragni, G. Radaelli, A. Maurichi, and R. Marchesini, "The ABCD system of melanoma detection: A spectrophotometric analysis of the asymmetry, border, color, and dimension," *Cancer*, vol. 85, no. 1, pp. 72–77, Jan. 1999.

[18] R. P. Braun, H. Rabinovitz, M. Oliviero, A. W. Kopf, J. H. Saurat, and L. Thomas, "Dermoscopy of pigmented skin lesions," *Annales De Dermatologie Et De Venereologie*, vol. 129, no. 2, pp. 187–202, Feb. 2002.

[19] R. M. MacKie, C. Fleming, A. D. McMahon, and P. Jarrett, "The use of the dermatoscope to identify early melanoma using the three-colour test," *Brit. J. Dermatol.*, vol. 146, no. 3, pp. 481–484, Mar. 2002.

[20] V. McGovern, "Digital diagnosis: New tool for detecting skin cancer," *Environ Health Perspect.*, vol. 111, no. 14, pp. A770–A773, Nov. 2003.

[21] V. Narayanamurthy, P. Padmapriya, A. Noorasafrin, B. Pooja, K. Hema, A. Y. F. Khan, K. Nithyakalyani, and F. Samsuri, "Skin cancer detection using non-invasive techniques," *RSC Adv.*, vol. 8, no. 49, pp. 28095–28130, Aug. 2018.

[22] E. L. Psaty and A. C. Halpern, "Current and emerging technologies in melanoma diagnosis: The state of the art," *Clinics Dermatol.*, vol. 27, no. 1, pp. 35–45, Jan. 2009.

[23] V. Revathi and A. Chithra, "A review on segmentation techniques in skin lesion images," *Int. Res. J. Engg Tech.*, vol. 2, no. 9, 2015.

[24] S.-M. Hwang, H.-C. Pan, M.-K. Hwang, M.-W. Kim, and J.-S. Lee, "Malignant skin tumor misdiagnosed as a benign skin lesion," *Arch Craniofacial Surg.*, vol. 17, no. 2, p. 86, 2016.

[25] A. A. Adeyinka and S. Viriri, "Skin lesion images segmentation: A survey of the state-of-the-art," in *Proc. Int. Conf. Mining Intell. Knowl. Explor.* Cham, Switzerland: Springer, 2018, pp. 321–330.

[26] Y. Yuan and Y.-C. Lo, "Improving dermoscopic image segmentation with enhanced convolutional–deconvolutional networks," *IEEE J. Biomed. Health Inform.*, vol. 23, no. 2, pp. 519–526, Mar. 2019.

[27] R. C. Maron *et al.*, "Systematic outperformance of 112 dermatologists in multiclass skin cancer image classification by convolutional neural networks," *Eur. J. Cancer* vol. 119, pp. 57–65, Sep. 2019.

[28] N. C. F. Codella, Q.-B. Nguyen, S. Pankanti, D. A. Gutman, B. Helba, A. C. Halpern, and J. R. Smith, "Deep learning ensembles for melanoma recognition in dermoscopy images," *IBM J. Res. Develop.*, vol. 61, nos. 4–5, pp. 5-1–5-15, Jul. 2017.

[29] F. Warsi, R. Khanam, S. Kamya, and C. P. Suárez-Araujo, "An efficient 3D color-texture feature and neural network technique for melanoma detection," *Inform. Med. Unlocked*, vol. 17, Apr. 2019, Art. no. 100176.

[30] C. Barata, J. S. Marques, and T. Mendonça, "Bag-of-features classification model for the diagnose of melanoma in dermoscopy images using color and texture descriptors," in *Proc. Int. Conf. Image Anal. Recognit.* Berlin, Germany: Springer, 2013, pp. 547–555.

[31] G. Schaefer, B. Krawczyk, M. E. Celebi, and H. Iyatomi, "An ensemble classification approach for melanoma diagnosis," *Memetic Comput.*, vol. 6, no. 4, pp. 233–240, Dec. 2014.

[32] Z. Waheed, A. Waheed, M. Zafar, and F. Riaz, "An efficient machine learning approach for the detection of melanoma using dermoscopic images," in *Proc. IEEE Int. Conf. Commun., Comput. Digit. Syst. (C-CODE)*, Mar. 2017, pp. 316–319.

[33] S. Sivaraj, R. Malmathanraj, and P. Palanisamy, "Detecting anomalous growth of skin lesion using threshold-based segmentation algorithm and fuzzy K–Nearest Neighbor classifier," *J. Cancer Res. Therapeutics*, 2018.

[34] A. Pennisi, D. D. Bloisi, D. Nardi, A. R. Giampetruzzi, C. Mondino, and A. Facchiano, "Skin lesion image segmentation using delaunay triangulation for melanoma detection," *Computerized Med. Imag. Graph.*, vol. 52, pp. 89–103, Sep. 2016.

[35] L. Bi, J. Kim, E. Ahn, D. Feng, and M. Fulham, "Automatic melanoma detection via multi-scale lesion-biased representation and joint reverse classification," in *Proc. IEEE 13th Int. Symp. Biomed. Imag. (ISBI)*, Apr. 2016, pp. 1055–1058.

[36] O. Yıldız, "Melanoma detection from dermoscopy images with deep learning methods: A comprehensive study," *J. Fac. Eng. Archit. Gazi Univ.* vol. 34, no. 4, pp. 2241–2260, 2019.

[37] W. Abbes and D. Sellami, "Deep neural network for fuzzy automatic melanoma diagnosis," in *Proc. 14th Int. Joint Conf. Comput. Vis., Imag. Comput. Graph. Theory Appl.*, 2019, pp. 47–56, doi: 10.5220/0007697900470056.

[38] K. M. Hosny, M. A. Kassem, and M. M. Foaud, "Skin cancer classification using deep learning and transfer learning," in *Proc. IEEE 9th Cairo Int. Biomed. Eng. Conf. (CIBEC)*, Dec. 2018, pp. 90–93.

[39] A. Esteva, B. Kuprel, R. A. Novoa, J. Ko, S. M. Swetter, H. M. Blau, and S. Thrun, "Dermatologist-level classification of skin cancer with deep neural networks," *Nature*, vol. 542, no. 7639, pp. 115–118, 2017.

[40] B. Kong, S. Sun, X. Wang, Q. Song, and S. Zhang, "Invasive cancer detection utilizing compressed convolutional neural network and transfer learning," in *Medical Image Computing and Computer Assisted Intervention—MICCAI* (Lecture Notes in Computer Science). Cham, Switzerland: Springer, 2018.

[41] S. Wu, Z. Gao, Z. Liu, J. Luo, H. Zhang, and S. Li, "Direct reconstruction of ultrasound elastography using an end-to-end deep neural network," in *Medical Image Computing and Computer Assisted Intervention—MICCAI* (Lecture Notes in Computer Science: Lecture Notes in Artificial Intelligence and Lecture Notes in Bioinformatics). Cham, Switzerland: Springer, 2018.

[42] B. Kong, Y. Zhan, M. Shin, T. Denny, and S. Zhang, "Recognizing end-diastole and end-systole frames via deep temporal regression network," in *Medical Image Computing and Computer Assisted Intervention—MICCAI* (Lecture Notes in Computer Science: Lecture Notes in Artificial Intelligence and Lecture Notes in Bioinformatics). Cham, Switzerland: Springer, 2016.

[43] M. A. Al-Masni, M. A. Al-Antari, M.-T. Choi, S.-M. Han, and T.-S. Kim, "Skin lesion segmentation in dermoscopy images via deep full resolution convolutional networks," *Comput. Methods Programs Biomed.*, vol. 162, pp. 221–231, Aug. 2018.

[44] X. He, Z. Yu, T. Wang, B. Lei, and Y. Shi, "Dense deconvolution net: Multi path fusion and dense deconvolution for high resolution skin lesion segmentation," *Technol. Health Care*, vol. 26, pp. 307–316, May 2018.

[45] M. Goyal and M. H. Yap, "Multi-class semantic segmentation of skin lesions via fully convolutional networks," 2017, *arXiv:1711.10449*. [Online]. Available: https://arxiv.org/abs/1711.10449

[46] D. Ramachandram and T. DeVries, "LesionSeg: Semantic segmentation of skin lesions using deep convolutional neural network," 2017, *arXiv:1703.03372*. [Online]. Available: https://arxiv.org/abs/1703.03372

[47] Y. Li and L. Shen, "Skin lesion analysis towards melanoma detection using deep learning network," *Sensors*, vol. 18, no. 2, p. 556, Feb. 2018.

[48] M. Wu, X. Zhao, Z. Sun, and H. Guo, "A hierarchical multiscale super-pixel-based classification method for extracting urban impervious surface using deep residual network from worldview-2 and LiDAR data," *IEEE J. Sel. Topics Appl. Earth Observ. Remote Sens.*, vol. 12, no. 1, pp. 210–222, Jan. 2019.

[49] C. H. Sudre, W. Li, T. Vercauteren, S. Ourselin, and M. Jorge Cardoso, "Generalised dice overlap as a deep learning loss function for highly unbalanced segmentations," in *Deep Learning in Medical Image Analysis and Multimodal Learning for Clinical Decision Support*. Cham, Switzerland: Springer, 2017, pp. 240–248.

[50] J. Long, E. Shelhamer, and T. Darrell, "Fully convolutional networks for semantic segmentation," in *Proc. IEEE Conf. Comput. Vis. Pattern Recognit.*, Jun. 2015, pp. 3431–3440.

[51] T. Mendonca, P. M. Ferreira, J. S. Marques, A. R. S. Marcal, and J. Rozeira, "PH2—A dermoscopic image database for research and benchmarking," in *Proc. 35th Annu. Int. Conf. IEEE Eng. Med. Biol. Soc. (EMBC)*, Jul. 2013, pp. 5437–5440.

[52] N. Codella, V. Rotemberg, P. Tschandl, M. E. Celebi, S. Dusza, D. Gutman, B. Helba, A. Kalloo, K. Liopyris, M. Marchetti, H. Kittler, and A. Halpern, "Skin lesion analysis toward melanoma detection 2018: A challenge hosted by the international skin imaging collaboration (ISIC)," 2019, *arXiv:1902.03368*. [Online]. Available: https://arxiv.org/abs/1902.03368

[53] ISIC. (2017). *Challenge Results*. [Online]. Available: https://challenge.kitware.com/

[54] M. I. Razzak, S. Naz, and A. Zaib, "Deep learning for medical image processing: Overview, challenges and the future," in *Classification in BioApps*. Cham, Switzerland: Springer, 2018, pp. 323–350.

[55] C. Rasche, "Melanoma recognition with an ensemble of techniques for segmentation and a structural analysis for classification," 2018, *arXiv:1807.06905*. [Online]. Available: https://arxiv.org/abs/1807.06905

[56] R. C. Hardie, R. Ali, M. S. De Silva, and T. M. Kebede, "Skin lesion segmentation and classification for ISIC 2018 using traditional classifiers with hand-crafted features," 2018, *arXiv:1807.07001*. [Online]. Available: https://arxiv.org/abs/1807.07001

[57] M. R. Guarracino and L. Maddalena, "Segmenting dermoscopic images," 2017, *arXiv:1703.03186*. [Online]. Available: https://arxiv.org/abs/1703.03186

[58] M. Aljanabi, Y. Özok, J. Rahebi, and A. Abdullah, "Skin lesion segmentation method for dermoscopy images using artificial bee colony algorithm," *Symmetry*, vol. 10, no. 8, p. 347, Aug. 2018.

ADEKANMI A. ADEGUN received the B.Tech. degree in computer science from the University of Ibadan, Nigeria, and the M.Sc. degree from the Ladoke Akintola University of Technology, Ogbomosho. He is currently pursuing the Ph.D. degree in computer science with the University of KwaZulu-Natal, South Africa.

He is currently working on research in developing deep learning framework for medical image analysis with the School of Mathematics, Statistics and Computer Science, University of KwaZulu-Natal. He also works as a Lecturer with the Department of Computer Science, Landmark University, Nigeria. He has published some of his research works in some accredited *Computer Vision and Image Processing* journals, and international and national conference proceedings. His research areas include machine learning, computer vision, image processing, pattern recognition, and medical image analysis.

SERESTINA VIRIRI (Member, IEEE) is currently a Professor of computer sciences. He is also working as a Professor of the School of Mathematics, Statistics and Computer Science, University of KwaZulu-Natal, South Africa. He is an NRF-Rated Researcher. He has published extensively in several accredited *Computer Vision and Image Processing* journals, and international and national conference proceedings. His research areas include computer vision, image processing, pattern recognition, and other image processing related areas, such as biometrics, medical imaging, and nuclear medicine.

Prof. Viriri serves as a Reviewer for several accredited journals. He has served on program committees for numerous international and national conferences. He has graduated several M.Sc. and Ph.D. students.

● ● ●